Bioactive Materials 21 (2023) 313–323

Contents lists available at ScienceDirect

Bioactive Materials

journal homepage: www.keaipublishing.com/en/journals/bioactive-materials

Breathable, antifreezing, mechanically skin-like hydrogel textile wound dressings with dual antibacterial mechanisms

Sihan Jiang [a,c,1], Jiajia Deng [a,b,1], Yuhui Jin [c], Bo Qian [c], Wanqi Lv [a,b], Qiangqiang Zhou [b,d], Enhua Mei [a,b], Rasoul Esmaeely Neisiany [e], Yuehua Liu [a,b,***], Zhengwei You [c,**], Jie Pan [a,b,*]

[a] Department of Orthodontics, Shanghai Stomatological Hospital & School of Stomatology, Fudan University, Shanghai, 200001, PR China
[b] Shanghai Key Laboratory of Craniomaxillofacial Development and Diseases, Fudan University, Shanghai, 200001, PR China
[c] State Key Laboratory for Modification of Chemical Fibers and Polymer Materials, College of Materials Science and Engineering, Institute of Functional Materials, Research Base of Textile Materials for Flexible Electronics and Biomedical Applications (China Textile Engineering Society), Shanghai Engineering Research Center of Nano-Biomaterials and Regenerative Medicine, Donghua University, Shanghai, 201620, PR China
[d] Department of Endodontics, Shanghai Stomatological Hospital & School of Stomatology, Fudan University, Shanghai, 200001, PR China
[e] Department of Materials and Polymer Engineering, Faculty of Engineering, Hakim Sabzevari University, Sabzevar, 9617976487, Iran

ARTICLE INFO

Keywords:
Hydrogel textile
Hydrogel dressing
Breathable
Dual antibacterial
Skin regeneration

ABSTRACT

Hydrogels are emerging as the most promising dressings due to their excellent biocompatibility, extracellular matrix mimicking structure, and drug loading ability. However, existing hydrogel dressings exhibit limited breathability, poor environmental adaptability, potential drug resistance, and limited drug options, which extremely restrict their therapeutic effect and working scenarios. Here, the current research introduces the first paradigm of hydrogel textile dressings based on novel gelatin glycerin hydrogel (glyhydrogel) fibers fabricated by the Hofmeister effect based wet spinning. Benefiting from the unique knitted structure, the textile dressing features excellent breathability (1800 times that of the commercially available 3 M dressing) and stretchability (535.51 ± 38.66%). Furthermore, the glyhydrogel textile dressing can also withstand the extreme temperature of −80 °C, showing the potential for application in subzero environments. Moreover, the introduction of glycerin endows the textile dressing with remarkable antibacterial property and expands the selection of loaded drugs (e.g., clindamycin). The prepared glyhydrogel textile dressing shows an excellent infected wound healing effect with a complete rat skin closure within 14 days. All these functions have not been achievable by traditional hydrogel dressings and provide a new approach for the development of hydrogel dressings.

1. Introduction

Skin is considered as the largest organ and the main external defense system of the human body, which protects the human body from microbial infection and external environmental damage, and also plays an important role in regulating body temperature and sensing external stimuli [1–5]. However, owing to various factors including inflammation and infections, etc., the healing process of injured skin does not proceed in an orderly manner, which results in a long healing time [6]. Wound dressings provide a physical barrier between the wound and the external environment to prevent further injury and infection, while also directing the reorganization of skin cells and subsequent infiltration and integration of host tissues, which is an effective means to promote skin tissue repair [7]. An ideal wound dressing should

Peer review under responsibility of KeAi Communications Co., Ltd.

* Corresponding author. Department of Orthodontics, Shanghai Key Laboratory of Craniomaxillofacial Development and Diseases, Shanghai Stomatological Hospital & School of Stomatology, Fudan University, Shanghai, 200001, PR China.

** Corresponding author. State Key Laboratory for Modification of Chemical Fibers and Polymer Materials, College of Materials Science and Engineering, Institute of Functional Materials, Research Base of Textile Materials for Flexible Electronics and Biomedical Applications (China Textile Engineering Society), Shanghai Engineering Research Center of Nano-Biomaterials and Regenerative Medicine, Donghua University, Shanghai, 201620, PR China.

*** Corresponding author. Department of Orthodontics, Shanghai Key Laboratory of Craniomaxillofacial Development and Diseases, Shanghai Stomatological Hospital & School of Stomatology, Fudan University, Shanghai, 200001, PR China.

E-mail addresses: liuyuehua@fudan.edu.cn (Y. Liu), zyou@dhu.edu.cn (Z. You), jiepan@fudan.edu.cn (J. Pan).

[1] Sihan Jiang and Jiajia Deng contributed equally to this work.

https://doi.org/10.1016/j.bioactmat.2022.08.014
Received 12 July 2022; Received in revised form 17 August 2022; Accepted 17 August 2022

meet the following requirements, including antibacterial, biocompatibility, favorable breathability, suitable mechanical properties, and providing appropriate physiological conditions to promote cell growth [8]. Varieties of dressings have been developed to promote wound repair, including traditional gauze, bandages, as well as newly developed rubbers, films, nanofibers, foams, and hydrogels [9,10]. Among these wound dressings, hydrogels have become the most competitive candidate due to drug delivering capabilities, high porosity, and extracellular matrix mimicking properties [11–14]. However, hydrogels are sensitive to the external environment and susceptible to changing the material properties due to the evaporation and freezing of water in dry and subzero environments, losing their functionalities which limits their application [15–17]. Moreover, most of the currently developed hydrogel dressings are used in the form of films with poor breathability, which restrict the penetration of oxygen toward the wound and even lead to inflammation after wearing for a long time [18,19]. High porosity and breathability are the advantages of textile dressings, which provide a suitable environment for wound healing [20–23]. Compared with other forms of dressings, textiles possess excellent stretchability and cushioning against pressure, which can better withstand the deformation and high tension of the skin [24]. Consequently, the combination of hydrogel and textile dressing can pave the path to overcome the previous shortcomings.

At present, Staphylococcus aureus (*S. aureus*) usually colonizes the skin surface and upper respiratory mucosa, causing a large proportion of skin wound infection [25], and the conventional treatment strategy is based on the usage of broad-spectrum antibiotics. Clinically, owing to the widespread use of broad-spectrum antibiotics, a large number of drug-resistant strains and mutant strains have emerged [26,27]. In addition, most of the loaded drugs in hydrogel dressing are water-soluble antibiotics. However, a single type of drug use can further exacerbate antibiotics side effects.

In this article, we developed a new type of wound dressing, glycerin hydrogel (glyhydrogel) textile, to address all the aforementioned challenges. This hydrogel textile combined the advantages of emerging hydrogel dressings and traditional gauze textile dressings. The unique knitted structures endowed the hydrogel textile dressing with remarkable breathability and stretchability [28]. Furthermore, glycerin, a widely used biocompatible icing inhibitor, was introduced into hydrogel textile dressings to inhibit the formation of ice crystals and resist the subzero temperature via forming strong hydrogen bonds with water molecules [29]. Furthermore, glycerin also endowed the hydrogel textile dressing with intrinsically bacteriostatic capacity and expanded the range of loaded antibiotics, especially lipid-soluble components. These features significantly enriched the medication strategy and improved the antibacterial property of the developed dressings with a great potential to alleviate serious drug resistance. Here, we set up an efficient way to fabricate the novel glyhydrogel textile dressings based on gelatin and demonstrated their excellent breathability, antifreezing property, favorable biological functions, and strong wound healing capability in an infected model.

2. Materials and method

2.1. Materials

Gelatin (type A, from porcine skin, 300 Bloom) and glycerin (≥99.0%) were purchased from Sigma-Aldrich. $(NH_4)_2SO_4$ (≥99.5%) was purchased from Titan (Shanghai), Inc. Glutaraldehyde (50% in H_2O) was supplied by Macklin. $Ca(NO_3)_2{\cdot}4H_2O$ (≥99.0%) was provided by Sinopharm Chemical Co. Ltd. Deionized water was used in the experiments. 3 M Tegaderm™ Hydrocolloid Thin Dressing (90022 T) was purchased from Minnesota Mining and Manufacturing Co. (Taiwan). Staphylococcus aureus was donated by the School of Pharmacy of Fudan University. Dulbecco's Modified Eagle's Medium (DMEM), fetal bovine plasma (FBS), phosphate buffered saline (PBS), and penicillin-streptomycin were all purchased from Gibco (Thermo Fisher Scientific, Inc.). The CCK-8 reagent was supplied by Beyotime (Shanghai, China). A Live/dead staining kit was obtained from Invitrogen Corporation (CA, USA). The L929 fibroblast cells were purchased from the National Collection of Authenticated Cell Cultures (Shanghai, China). All the reagents were used as received.

2.2. Fabrication of gelatin hydrogel fibers

A certain amount of gelatin powder (30 g) and $Ca(NO_3)_2{\cdot}4H_2O$ (5 g) were dissolved in deionized water (100 g) and stirred at 50 °C until the mixture became a homogeneous solution. The obtained gelatin solution were filled in a 20 mL syringe and extruded through a steel needle (18G) into a coagulating bath (ammonium sulfate aqueous solutions) at room temperature (25 °C), wherein the mass ratio between ammonium sulfate and water was 1:5. The flow rate of the solution was set at 80 mL/h utilizing a syringe pump (MP-2003, Leien Medical Equipment Co., Ltd, China) and the obtained fibers were continuously collected on a cylindrical winding bobbin at a line speed of 38 cm/min. After spinning, the collected fibers were subsequently immersed in the same concentration of ammonium sulfate aqueous solutions for 12 h to displace the solvent.

For gelatin hydrogel fibers not treated with ammonium sulfate and glutaraldehyde, they were fabricated by squeezing a certain amount of gelatin solution through a steel needle (18G) into a watch glass and placed in the refrigerator for 30 min for gelation.

2.3. Fabrication of crosslinked gelatin hydrogel and glyhydrogel fibers

The prepared gelatin hydrogel fibers were put into a glutaraldehyde-containing ammonium sulfate aqueous solution at room temperature for 12 h to synthesize the crosslinked gelatin hydrogel fibers. After rinsing with deionized water 3 times, the crosslinked gelatin hydrogels were then soaked in a mixed solution made of glycerin and ammonium sulfate aqueous solution to prepare crosslinked gelatin glyhydrogel fibers, wherein the mass ratio among glycerin, ammonium sulfate, and water was set at 11:1:10. For comparison, the crosslinked gelatin hydrogel fibers were also prepared in the same process using solely ammonium sulfate aqueous solution without glycerin.

To facilitate further discussion, the gelatin hydrogel fibers and glyhydrogel fibers were defined as F-N_xW_yG and F-N_xW_y, respectively, where F–N_0W_0 represented gelatin hydrogel fibers neither treated with ammonium sulfate nor crosslinked with glutaraldehyde. "F", "N", "W" and "G" represented fiber, ammonium sulfate, glutaraldehyde, and glycerin respectively, "x" corresponded to the concentration of $(NH_4)_2SO_4$ solution used in crosslinking reaction and solvent displacement, while "y" represented the concentration of glutaraldehyde used in crosslinking reaction. The mass fraction of glycerin in the mixed soaking solution was 50%. The various formula of reaction solutions for preparing crosslinked gelatin hydrogel fibers were summarized in Table 1.

2.4. Fabrication of gelatin glyhydrogel film dressing

A certain amount of gelatin powder (30 g) and $Ca(NO_3)_2{\cdot}4H_2O$ (5 g) were dissolved in deionized water (100 g) and stirred at 50 °C until the mixture became a homogeneous solution. The obtained gelatin solution (5 mL) was squeezed into a watch glass and placed in the refrigerator for 30 min for gelation, and then the gelled gelatin hydrogel film was put into a glutaraldehyde-containing ammonium sulfate aqueous solution at

Table 1
Formulas of reaction solution for preparing crosslinked hydrogel fibers.

Sample code	Fiber	$(NH_4)_2SO_4$	Glutaraldehyde	H_2O
F–$N_{10}W_{0.2}$	1.00 g	6.67 g	0.13 g	66.67 g
F–$N_{10}W_{0.6}$	1.00 g	6.67 g	0.40 g	66.67 g
F–$N_{10}W_1$	1.00 g	6.67 g	0.67 g	66.67 g

room temperature for 12 h to synthesize the crosslinked gelatin hydrogel. After 3 times rinsing with deionized water, the crosslinked gelatin hydrogel films were then soaked in a mixed solution made of glycerin and ammonium sulfate aqueous solution to prepare crosslinked gelatin glyhydrogel film, wherein the mass ratio among glycerin, ammonium sulfate, and water was set at 11:1:10.

2.5. Fabrication of glyhydrogel textile dressing

The prepared hydrogel fibers were knitted into a wound dressing using knitting needles (diameter 2.5 mm), followed by the crosslinking process with the same procedure as that of preparing crosslinked gelatin glyhydrogel fibers.

To facilitate further discussion, the gelatin glyhydrogel films dressings and glyhydrogel textile dressings were defined as D-GF and D-GT respectively, where “D”, “G”, “F” and “T” represented dressings, glyhydrogels, films, and textiles respectively. The various formula of reaction solutions for preparing D-GF and D-GT were summarized in Table 2.

2.6. Characterizations

The chemical structures were evaluated by using attenuated total reflection Fourier transform infrared (ATR-FTIR). The tensile tests and cyclic tensile tests were performed on the MTS E42 machine. The air permeability of the prepared dressings was assessed according to GB/T5453:1997 by an air permeability tester under different pressures. A differential scanning calorimeter (DSC) was employed for the DSC tests. The stability of hydrogel fibers with different crosslinking densities were evaluated in a 37 °C water bath. The experimental details are available in Supporting Information.

2.7. Cytocompatibility of the hydrogel and glyhydrogel fibers

The cytotoxicity of two kinds of gel fibers was evaluated by direct contact between L929 cells and gels, and cell proliferation in gel suspension was accessed by the CCK-8 method. The experimental details are available in Supporting Information.

For the cell proliferation tests, hydrogel and glyhydrogel fibers were soaked in a complete medium (0.1 g/mL) to prepare the suspension. The 3×10^5/mL cell suspensions were prepared in advance. The experimental details are available in Supporting Information.

2.8. Drug loading and release experiments

The loading and release profile of clindamycin from glyhydrogel fibers were studied *in vitro*. The experimental details are available in Supporting Information.

2.9. In vitro antibacterial studies on hydrogel and glyhydrogel fibers

Staphylococcus aureus (*S. aureus*. ATCC 29213) was selected to assess the antibacterial ability of hydrogel fibers, glyhydrogel fibers, and clindamycin-loaded glyhydrogel fibers. The experimental details are available in Supporting Information.

Table 2
Formulas of the reaction solution used for preparing crosslinked gelatin glyhydrogel film and glyhydrogel textile dressings.

Samples	Hydrogel	$(NH_4)_2SO_4$	Glutaraldehyde	H_2O
D-GF	5.80 g	20.00 g	1.20 g	200.00 g
D-GT	1.00 g	6.67 g	0.40 g	66.67 g

2.10. In vivo biocompatibility evaluation

All animals involved in this study were housed in an SPF room and were adapted to the new environment for one week before the experiment. During the studies, the temperature of the animal room was controlled at 24 °C, 12 h light, and dark daily cycle, and all animals ate freely. All procedures were performed following the guidelines issued by the Animal Care and Use Committee of Shanghai Shengchang Biotechnology Co., Ltd (ethical code:2021-09-KQ-PJ-008).

2.11. In vivo toxicity test

6-week-old SD rats were implanted subcutaneously with various dressings to observe inflammatory cells. The experimental details are available in Supporting Information.

2.12. Infected full-thickness skin wound healing assessment

Infectious full-thickness wounds were used for the evaluation of the performance of hydrogels in wound healing. The experimental details are available in Supporting Information.

2.13. Histological analysis

On days 3, 7, and 14, the regenerated skin tissues were harvested at different times. All samples were immersed in 4% PFA and fixed overnight, dehydrated in gradient alcohol, embedded in paraffin, and sectioned (6 μm in thickness). Some sections were stained with H&E, Masson trichrome to observe collagen fiber, and immunofluorescence staining to evaluate blood vessel regeneration. The harvested sections were incubated with CD31 and α-SMA primary antibodies overnight. The nuclei were stained with DAPI, and the samples were observed under a fluorescence microscope (Leica, Germany).

3. Results and discussion

3.1. Preparation and characterization of hydrogel and glyhydrogel fibers

Gelatin is a natural polymer with excellent biocompatibility, which has been widely used as the raw material for hydrogels [30–32]. However, the natural gelation of gelatin aqueous solutions is a time- and temperature-dependent process that lacks controllability and is difficult to match with the fast-spinning processes. Although the addition of photo-crosslinking components can partially address the problem, it mostly compromises the biocompatibility of the gel. Consequently, up to now, no effective method has been reported in the continuous preparation of pure gelatin-based hydrogel fibers. By exploiting the Hofmeister effect, the effect of inorganic salts on the solubility of proteins in water, we achieved the continuous spinning of pure gelatin-based hydrogel fibers by adding two inorganic salts ($Ca(NO_3)_2$ and $(NH_4)_2SO_4$) to tailor the interaction between gelatin and water molecules (Fig. 1a). The spinning solutions were prepared by dissolving a certain amount of gelatin and $Ca(NO_3)_2$ powders in water. The incorporation of $Ca(NO_3)_2$ (chaotropes) increased the hydrated water content of gelatin molecules and inhibited the formation of hydrogen bonds between gelatin chains, thus delaying the gelation of gelatin aqueous solution at room temperature and resulting in smooth extrusion of the gelatin aqueous solution [33]. Subsequently, the spinning solutions were squeezed into the $(NH_4)_2SO_4$ (kosmotropes) aqueous solution through a syringe pump. The strong interaction between $(NH_4)_2SO_4$ and water reduced the hydration water content of the gelatin molecules, contributing to the hydrophobic folding of the gelatin molecular chain and accelerating the formation of hydrogen bond between carbonyl and amine groups. This procedure resulted in rapid gelation of the gelatin aqueous solution and continuous spinning of gelatin hydrogel fibers. Compared with gelatin hydrogel fibers without incorporating

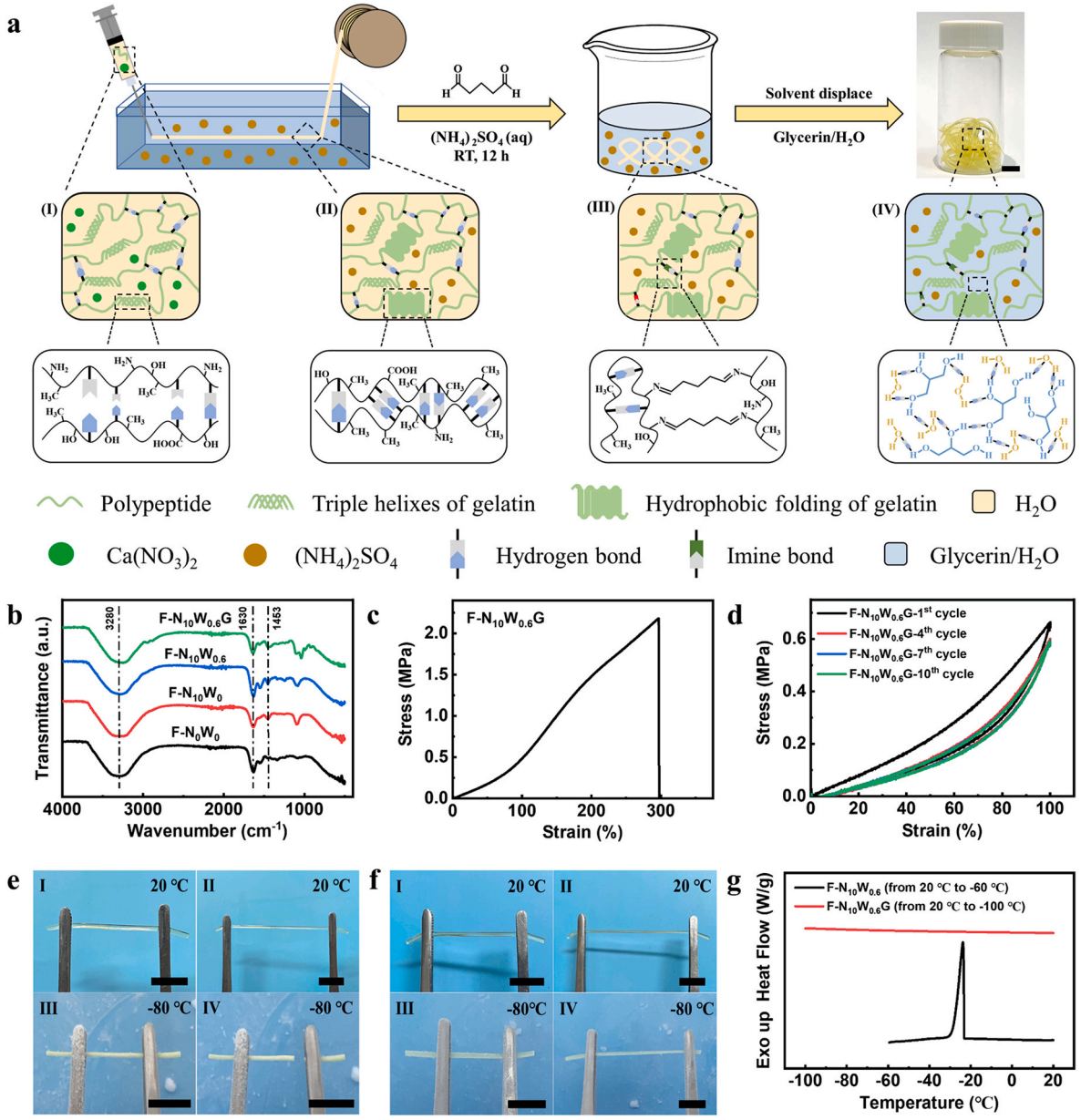

Fig. 1. Fabrication and characterization of crosslinked glyhydrogel fibers. (a) Schematic of the wet spinning process and molecular evolution of glyhydrogel fibers. Figure I-Ⅳ showed the structural evolution during the fabrication stages including (I) spinning solution, (II) hydrogel fiber, (III) crosslinked hydrogel fiber and (Ⅳ) crosslinked glyhydrogel fiber. Scale bar: 10 mm. (b) FTIR spectra of the prepared hydrogel and glyhydrogel fibers. (c) Typical tensile stress-strain curves of glyhydrogel fibers. (d) Cyclic tensile stress–strain curves of glyhydrogel fiber. (e–f) Photographs of (e) hydrogel and (f) glyhydrogel fibers stretched at 20 °C (I, II) and −80 °C (III, Ⅳ), respectively. Hydrogel fiber was frozen and easily broken while glyhydrogel fiber maintained stretchability at −80 °C after 24 h. Scale bars: 10 mm. (g) The DSC thermograms of the hydrogel and glyhydrogel fibers.

$(NH_4)_2SO_4$ (named F–N_0W_0), the enhanced intensity of C–H bond bending vibrations and CH_3 symmetrical deformation vibrations at 1453 cm^{-1} in Fourier transform infrared spectroscopy (FTIR) of hydrogel fibers incorporating $(NH_4)_2SO_4$ (named F–$N_{10}W_0$) indicated the formation of strong hydrophobic interaction (Fig. 1b) [34,35].

However, the obtained hydrogel fibers are temperature-sensitive and would rapidly re-transform from gel to solution above the gelation temperature (30 °C) or in an aqueous environment [36]. Crosslinking is an effective strategy to improve the stability of gelatin hydrogels. Through the Schiff reaction between the glutaraldehyde and the amine groups, covalent crosslinks containing imine bonds were introduced into the polymer network (F–$N_{10}W_{0.6}$, Table 1). As can be discerned from Fig. 1b, the crosslinking bonds increased the intensity of the amide I band at 1630 cm^{-1}, resulting from C═N stretching vibrations [37]. In order to optimize the crosslinking formula, hydrogel fibers with different crosslink densities were immersed in the water bath (37 °C) to assess their stability. The hydrogel fibers with medium (named F–$N_{10}W_{0.6}$) and high (named F–$N_{10}W_1$) degree of crosslinking remained stable after 7 days, whereas the lightly crosslinked glyhydrogel fibers (named F–$N_{10}W_{0.2}$) gradually dissolved after 12 h and completely disappeared after 24 h (Fig. S1). Considering the potential toxicity of high concentration of glutaraldehyde, F–$N_{10}W_{0.6}$ were selected for further studies. The subsequent solvent displacement converted the crosslinked hydrogel fibers into crosslinked glyhydrogel fibers (named F–$N_{10}W_{0.6}$G). The mass fraction of glycerin in F–$N_{10}W_{0.6}$G reached more than 41.0% ± 1.5% and the strong hydrogen bond formed between glycerin, water, and polymer network enhanced the intensity of the hydroxyl group stretching vibrations at 3280 cm^{-1} (Fig. 1b) [38]. The

obtained fibers featured excellent mechanical properties, with tensile strength, Young's modulus, and maximum elongation of 2.17 ± 0.22 MPa, 0.36 ± 0.03 MPa, and 297.42 ± 14.84%, respectively (Fig. 1c). Moreover, the stress-strain curves of the cyclic tensile test of glyhydrogel fibers showed negligible hysteresis (Fig. 1d), indicating the remarkable elasticity of glyhydrogel fibers.

As mentioned above, hydrogel fibers, as a form of hydrogels, have extremely stringent requirements on the working environment. At subzero temperature, free water in hydrogel fibers freezes, resulting in the reduction of transparency of the material and loss of elasticity. As shown in Fig. 1e, after storing in −80 °C for 24 h, hydrogel fibers became opaque and readily broke when being stretched while glyhydrogel fibers maintained their stretchability (Fig. 1f), which can be assigned to the formation of strong hydrogen bonds between glycerin and water, reducing the interaction between water molecules [39,40]. In addition, differential scanning calorimetry (DSC) was employed to evaluate the antifreezing performance of hydrogel and glyhydrogel fibers (Fig. 1g). The sharp peak approximately centered at −24 °C on the DSC curve of hydrogel fiber corresponded to the freezing of water and the introduction of inorganic salts lowered the freezing point of the water [40]. However, there was no crystallization peak on the DSC thermogram of glyhydrogel fibers from −100 °C to 20 °C, demonstrating the excellent low-temperature resistance. These results showed the application potential of the prepared glyhydrogel fibers in subzero environments, and the dressings knitted by such fibers can adapt to extremely cold weather.

3.2. Biocompatibility and biodegradation of hydrogel and glyhydrogel fibers

Biocompatibility is a critical requirement for the application of materials in the biomedical field. In this study, L929 fibroblasts were inoculated on the surface of hydrogel and glyhydrogel fibers, and cultured for 3 days for live and dead cell staining. As presented in Fig. S2a, a large number of cells were attached to the surface of the hydrogel and glyhydrogel fibers, indicating that fibroblasts grew well after direct contact with both fibers without obvious cytotoxicity.

To further evaluate the cytocompatibility of glyhydrogel fibers, L929 cells were co-cultured with gel extract, and a CCK-8 assay was carried out on day 1, 3, 5, and 7. As shown in Fig. S2d, the number of cells in hydrogel and glyhydrogel groups was significantly higher on day 3 than on day 1, and gradually increased with time. The CCK-8 results showed that the cells grew well in the gel extract. In addition, after 3 and 7 days of cell culture, staining results of living and dead cells showed that more than 95% cells expressed green fluorescence (Fig. S2b), and the survival rate of cells in the glyhydrogel group was higher than that in the hydrogel group (Fig. S2c). The above experimental results indicated that both gel fibers had excellent biocompatibility and wide application prospect in wound dressing.

We further implanted glyhydrogel fibers subcutaneously in rats to evaluate their biodegradation and biocompatibility. *In vivo* test was divided into three parts, including skin local inflammatory cell detection, blood biochemical detection, and histological detection of different organs, as presented in Fig. S3a. The sections showed that the glyhydrogel fibers were wrapped by fibrous tissue under the skin, and there were no obvious abnormalities in the surrounding tissue structure and no skin bleeding or ulceration (Fig. S3b). In all blood biochemical indexes, such as blood urea nitrogen (BUN), alkaline phosphatase (ALP), alanine transaminase (ALT), and uric acids (UA), the implanted glyhydrogel fibers showed no significant changes compared with the blank control group, and all indexes were within the normal ranges (Fig. S3c). Finally, no pathological changes were observed by comparing biopsies of the heart, liver, spleen, lung, and kidney (Fig. S3d). The results showed that the glyhydrogel fibers implanted subcutaneously had no obvious toxic and side effects on the blood and organs of rats, confirming their excellent biocompatibility.

3.3. Drug release and antibacterial property of hydrogel and glyhydrogel fibers

To mitigate the threat of antibiotic resistance to global health, scientists are working to develop non-antibiotic antimicrobials, of which glycerin has been reported to have antimicrobial effects *in vitro* [41]. As another limitation, the previously reported hydrogel dressings are only capable to dissolve water-soluble antibiotics.

Herein, we introduced glycerin to the dressing matrix not only endow it with intrinsically antibacterial property, but also enable the loading of lipid-soluble antibiotics. Regarding the antibacterial mechanism of glycerin, we believe that the following factors are involved in this process. Most organisms need to live in a water environment. The introduction of glycerin reduces the water content available for the bacterial cells. As a result, bacteria will dehydrate, dormant and die. Moreover, the glycerin permeates cells while preventing water from flowing out of the cells, which results in the increased osmotic pressure and the weakened membrane and cellular lysis, thus exhibit a bacteriostatic effect [42]. The antibacterial effect of this glycerin and antibiotics is considered to be a dual antibacterial effect. In clinical application, choosing appropriate methods according to different scenarios will help solve the problem of antibiotic abuse and drug resistance. Lipid-soluble drugs can fuse with the phospholipid bilayer of cell membranes, making them more readily absorbed and metabolized. Clindamycin (DA) is a common lipid-soluble antibiotic that is effective to treat infections caused by *S. aureus*. Damage repair requires long-term action of drugs at the site of injury. By loading and sustained release of clindamycin, glyhydrogel dressings would exhibit long-term anti-infection effects and promote wound healing. The release profile of clindamycin from the glyhydrogel fibers was evaluated in phosphate buffered saline (PBS) at pH 7.4. The release behavior of clindamycin in the first 8 h was almost linear (Fig. 2a, Table S1). Furthermore, the glyhydrogel fiber (F–$N_{10}W_{0.6}$G) continuously released clindamycin for more than 24 h, which was highly desirable for long-term bacterial inhibition effect during the healing process of skin wounds. At 1, 2, 4, 8 and 24 h, clindamycin was released 20.97 ± 0.54%, 29.30 ± 0.71%, 39.76 ± 0.51%, 51.96 ± 0.59% and 64.82 ± 0.42%, respectively. In a pH 7.4 solution, clindamycin was slowly released from the fibers and dissolved in PBS. Therefore, in chronically infected wounds, dressing came into contact with the tissue exudates and released the clindamycin into the fluid to diffuse around the wound to provide sustained bacteriostatic action.

Skin is the most superficial tissue of the human body, thereby, it is easy for *S. aureus* to colonize wounds [43]. Therefore, in this study, we applied clindamycin to improve the antibacterial performance of wound dressings. In this experiment, we firstly extracted the suspension released by glyhydrogel fibers. Afterward, we used suspension to culture bacteria for 24 h to observe whether there was colony formation. The experiment was divided into the normal medium group, hydrogel fiber group (F–$N_{10}W_{0.6}$), glyhydrogel fiber group (F–$N_{10}W_{0.6}$G), and DA-loaded glyhydrogel fiber group (F–$N_{10}W_{0.6}$G-DA). As shown in Fig. 2b, the bacteria treated with a normal medium grew well on the agar plate with a round shape colony and a golden yellow color. In the F–$N_{10}W_{0.6}$ group, a small amount of *S. aureus* colonies could be observed. However, no colony was formed on the agar plate in the F–$N_{10}W_{0.6}$G and F–$N_{10}W_{0.6}$G-DA groups. The results of the bacterial cloning experiment were consistent with the data of bacterial Live/dead staining, and the bacterial survival rates were determined to be 99.51 ± 0.23%, 29.26 ± 5.41%, 1.22 ± 0.26%, and 0.35 ± 0.18%, respectively (Fig. 2d and e). In another experiment, to quantitatively evaluate the antibacterial range of fibers, the agar diffusion method was employed to detect the antibacterial ring size. As shown in Fig. 2c, antibacterial rings appeared in both fibers, and the range of antibacterial rings in the F–$N_{10}W_{0.6}$G-DA (15.73 ± 0.87 mm) was significantly larger than that in the F–$N_{10}W_{0.6}$G (8.3 ± 0.43 mm) with a significant statistical difference ($P < 0.05$). The above results confirmed that the glyhydrogel fibers were

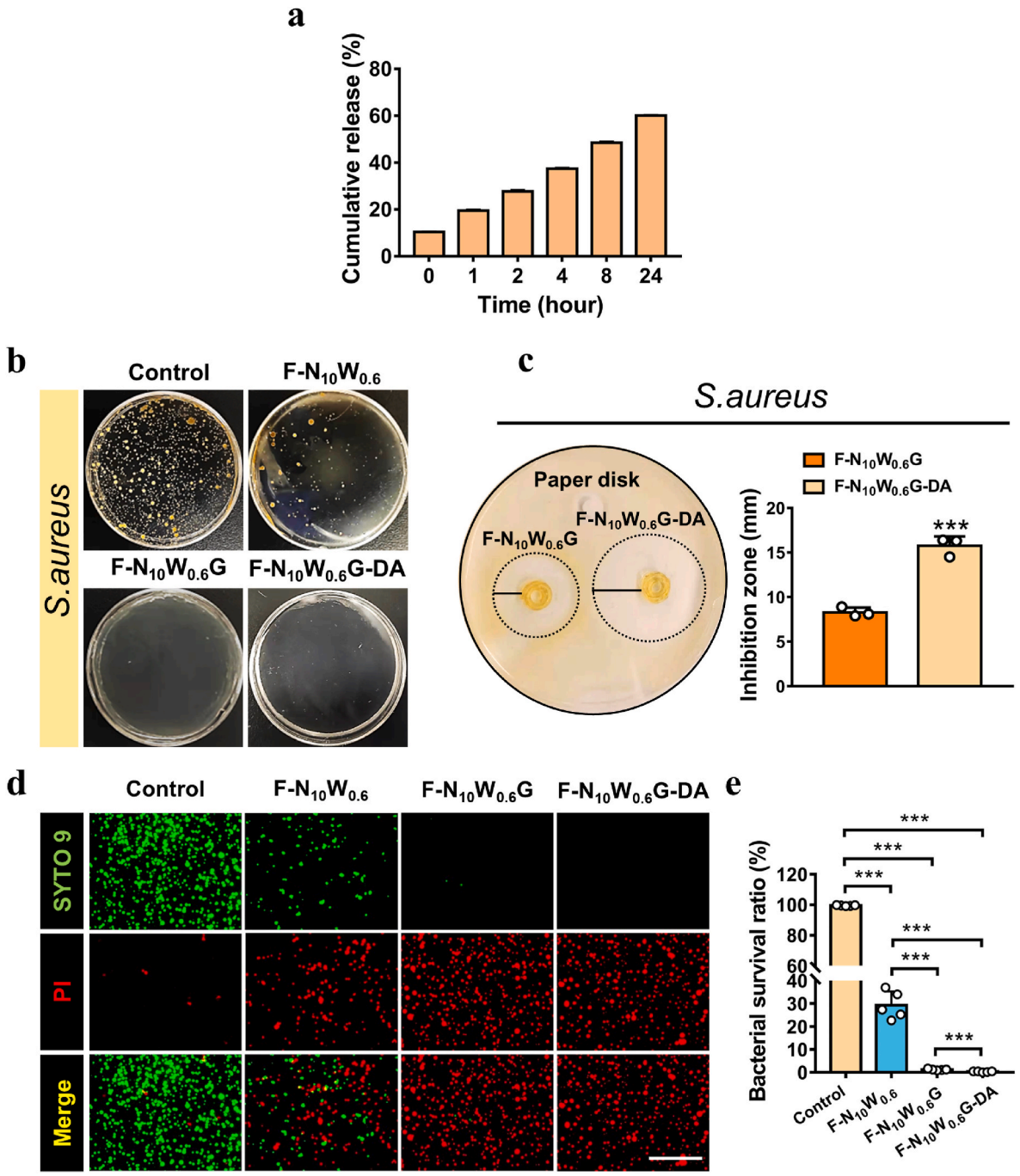

Fig. 2. Drug release and antibacterial study of the hydrogel and glyhydrogel fibers. (a) The Clindamycin release from glyhydrogel fiber was measured by collecting the released buffer over a period of 1–24 h. (b) Representative photographs of *S. aureus* colony growth on the agar plates for 24 h. (c) Photographs of antibacterial zones of *S. aureus* around glyhydrogel fibers and clindamycin loaded glyhydrogel fibers, statistical diagram of antibacterial area (n = 3). (d) The fluorescent microscopy images of the stained samples. *S. aureus* was incubated with different gel extracts for 48 h, and the bacteria were stained by Live/dead regent. Scale bars: 10 μm. e) The bacterial survival ratio of each groups. $^{***}P < 0.001$.

a promising candidate for preparing the dressings with intrinsically antibacterial property, which can be applied to infected wounds by themselves. The development of this non-antibiotic bacteriostatic material will help solve the problems of antibiotic abuse and drug resistance in clinical practice. And the loaded clindamycin significantly enhanced the antibacterial property of glyhydrogel textile dressings, which was expected to be applied to large-area infected and refractory infected wounds. The powerful antibacterial effect can significantly shorten the medication time, reduce the pain and economic burden of patients, and can be extended to other fields to improve the therapeutic effect. Such as the preparation of oral ulcer patches and artificial flexible skin.

3.4. Mechanical properties and air permeability of dressings

An ideal wound dressing must possess certain mechanical properties to ensure it will not rupture when suffering from bump or tear [44]. Since the excellent mechanical properties of the prepared glyhydrogel fibers, they can be readily knitted into textiles for use as dressings (Fig. 3a), which were further demonstrated to withstand different

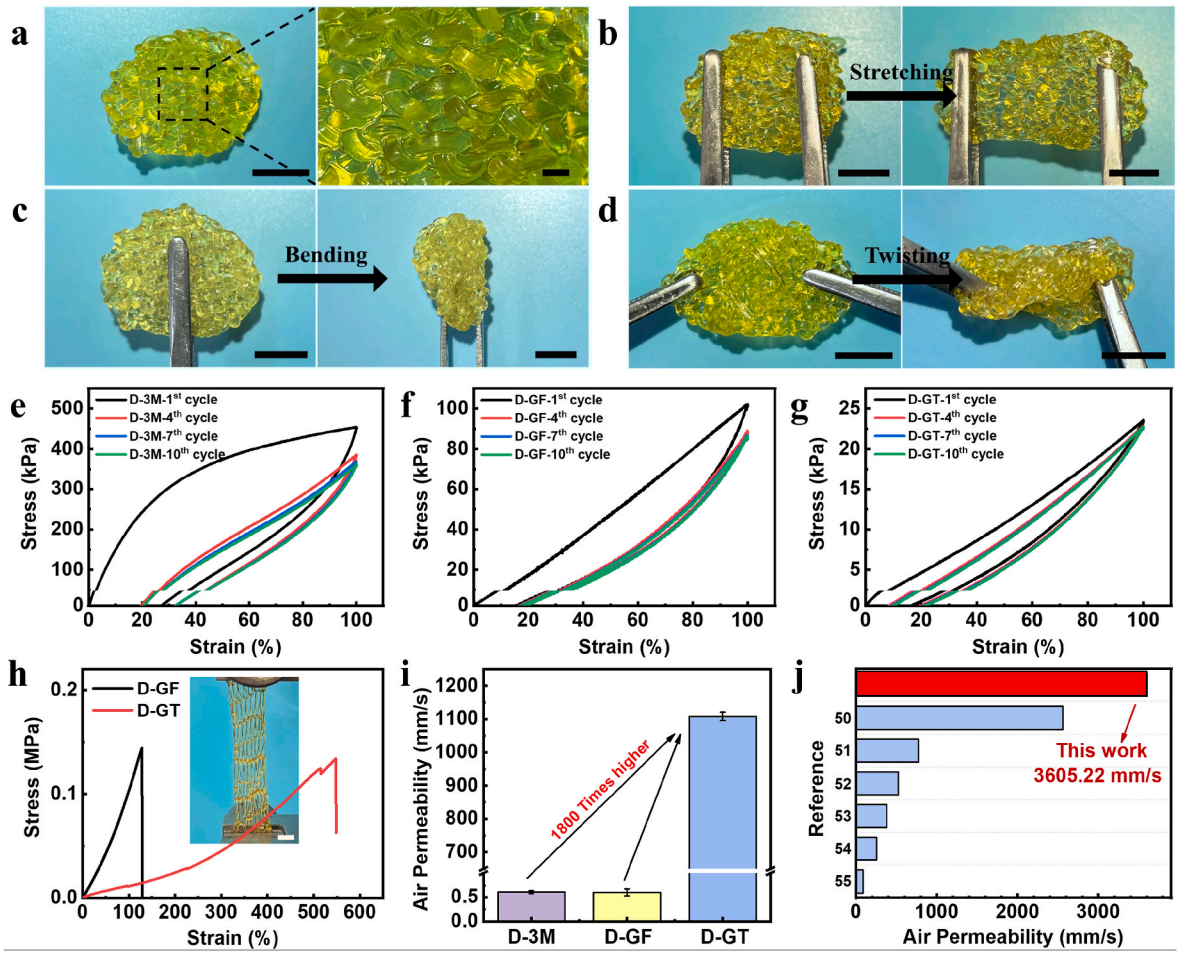

Fig. 3. Evaluation of the mechanical properties and air permeability of dressings. (a–d) (a) Photograph of glyhydrogel textile dressing and withstanding of the textile dressing under several modes of deformation including (b) stretching, (c) bending, and (d) twisting. Scale bars: 10 mm. (e–g) Cyclic tensile stress–strain curves of (e) D-3M, (f) D-GF, and (g) D-GT. (h) The typical tensile stress–strain curves of D-GT and D-GF. The inserted photograph was the stretched D-GT under tensile test. Scale bar: 10 mm. (i) The air permeability of D-3M, D-GF, and D-GT under 100 Pa. (j) The air permeability of D-GT and other dressings reported in the literature [50–55].

deformations including stretching, bending, and twisting (Fig. 3b–d). For the convenience of discussion, the glyhydrogel textile, glyhydrogel film, and commercially available 3 M dressing were named as D-GT, D-GF, and D-3M, respectively (Table 2). The cyclic tensile curve at 100% strain of D-3M showed an obvious hysteresis loop (Fig. 3e), while D-GF showed favorable elasticity in the cyclic tensile test (Fig. 3f), which attributed to the 3D network with multiple non-covalent interactions inside the glyhydrogel. The D-GT knitted by glyhydrogel fibers combined the advantages of hydrogel and textiles, featuring negligible hysteresis after 10 cycles according to the stress–strain curves (Fig. 3g), indicating the best elasticity among three different kinds of dressings. Moreover, benefiting from the dispersion of stress by the knitted structure [45], D-GT showed the ability to stretch surpass 5 times its original length, which was 4 times higher than D-GF dressing while having a similar tensile strength (Fig. 3h, Table S2). These mechanical properties provided the withstanding deformation during practical applications. In addition, the D-GT featured low Young's modulus (0.03 ± 0.01 MPa), which was similar to soft tissues in the human body (0.001–0.1 MPa) [46,47], resulting in a better adapt to the human skin [48].

Breathability, another crucial characteristic of wound dressing, was measured according to GB/T5453:1997. As can be discerned from Fig. 3i, the air permeability of D-3M (0.61 ± 0.03 mm/s) was almost the same as D-GF (0.60 ± 0.07 mm/s) under the pressure of 100 Pa. However, under the same conditions, the air permeability of D-GT reached up to 1107.78 ± 12.30 mm/s, which was more than 1800 times that of the other two dressings (Table S3). This excellent breathability was attributed to the highly porous knitted structures [49], which allowed sufficient oxygen concentration in the wound, thereby hindering the anaerobic bacteria growth and reproduction, keeping the wound dry, and constructing a niche conducive to tissue regeneration. We also measured the air permeability of the dressing under different pressures. The results showed that the gas content transmitting through dressing per unit time increased with the pressure, reaching up to 3605.22 ± 8.26 mm/s under the pressure of 500 Pa (Table S3), which featured the highest level of breathability among the reported hydrogel dressings and even comparable to gauze (Fig. 3j) [50–55].

3.5. *Wound healing effects of dressings in vivo*

In the case of living in cold or plateau areas, repeated wound infection often occurs due to the extreme environment and poor cold resistance of conventional wound dressings. The design of sustainable effective and biocompatible antifreezing wound dressings for refractory wounds in patients in extreme regions remains a clinical challenge. Wound healing is a complex physiological process, generally divided into four stages, and each stage has a specific physiological process. It includes hemostasis, inflammation limitation, cell proliferation, and remodeling [56]. Certain environmental stimuli alter the normal wound healing process, causing a delay in wound healing and resulting in chronic wounds that do not heal for more than 6 weeks. The wound dressing developed in this study not only had antibacterial ability, but was also beneficial to promote wound healing. The addition of glycerin

increased the frost resistance, making them suitable for application in even cold areas.

To assess the therapeutic effect of D-GT *in vivo*, we established a full-thickness skin wound model with *S. aureus* infection. The wound was covered with a dressing after infection, and the healing process was shown in Fig. 4a. The experiment was divided into five groups, including the untreated control group, D-3M, D-GF, D-GT, and DA-loaded glyhydrogel textile dressings (D-GT-DA). For the control group, after 3 days of infection, dark red inflammatory exudate and pseudo-membrane were observed around the wound margin, and the wound did not shrink. After covering dressing for 3 days, wound healing was significantly improved in all dressing groups compared to the control group (Fig. 4b and c) and there was no obvious inflammatory cells exudate around the wound. From day 3 to day 7, the infected wound healing of the control group was poor, while the wound healing rate of the D-GT-DA was over 70%, which was remarkably higher in comparison to the other groups (Fig. 4d and e). By day 14, the D-GT-DA had almost completely healed (wound closure was 98.85 ± 0.49%), while the wound of D-3M, D-GF, and D-GT did not heal completely. These experimental results proved that the drug-loaded dressings had the strongest killing effect on bacteria in the skin wound, while the dressing without drug loading also had the function of promoting wound healing, which may benefit from the strong moisturizing and physical protection of glycerin.

After skin samples were collected, H&E and Masson staining were performed to assess skin tissue healing at different time points. Rat normal skin consists of epidermis, dermis and subcutaneous tissue, and includes hair follicles, sebaceous glands and sweat glands (Fig. S4). As shown in Fig. S5a, there was infiltration of inflammatory cells on the skin surface and a lack of epidermal layer in the control and the D-3M group. However, there were no obvious inflammatory cells on the skin surface of glyhydrogel dressing group, indicating that glyhydrogel itself has certain bacteriostatic properties. Compared with normal skin

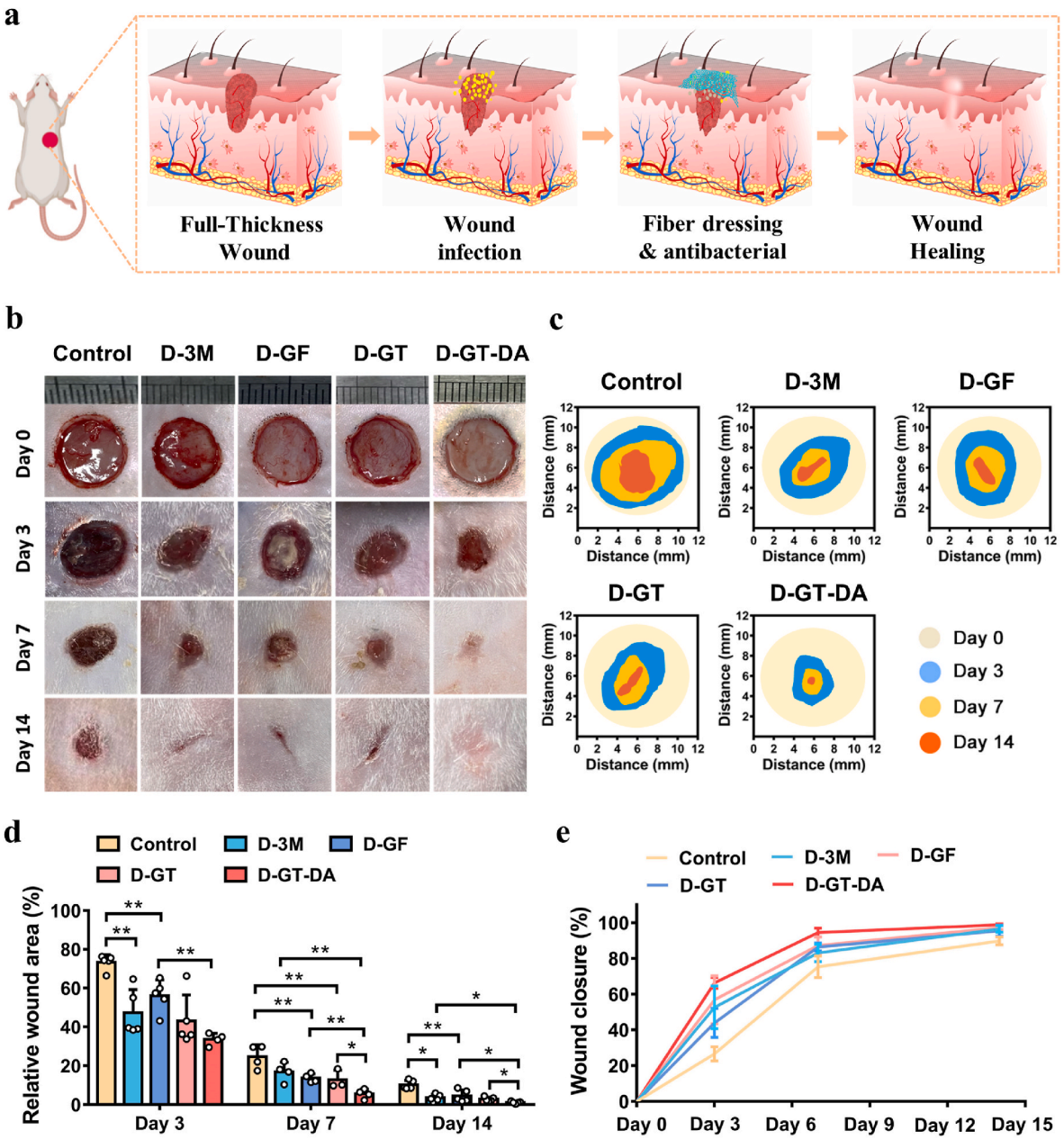

Fig. 4. *In vivo* infected full-thickness wound healing. (a) Schematic illustrations of the healing process of infected skin wounds. (b) Representative wound healing photographs of different dressings treated over 14 days. (c) Schematic images of wound contraction on day 0, 3, 7, and 14 after wound treatment. (d–e) The relative value of different dressing groups of remaining wounds and skin healing rate (n = 5). $^{*}P < 0.05$, $^{**}P < 0.01$.

structure, the wounds of all rats on day 3 lacked glandular and hair follicle structures, and the new epidermal layer lacked papillae structure. On day 7 (Fig. S5b), new tissue was formed on the surface of the wound covered with dressing in all four groups, and an epiderm-like structure was formed in the D-GT-DA, while the control surface was only covered by connective tissue. As shown in H&E staining, a few gland-like structures were observed subcutaneously in the D-GT group. However, only in the D-GT-DA group, a more mature sweat gland structure had been formed, and the morphology was similar to the normal skin structure. It showed that the wound healing rate of the D-GT and D-GT-DA groups was significantly faster than the other three groups, and the D-GT-DA group had the best healing effect. These results indicated that preventing infection early, dressing wounds timely and blocking environmental stimulus factors were the keys to promote skin healing.

Moreover, according to the healing results on day 14, no skin appendages and hair follicles were generated in the new tissue of the control and D-3M groups. In the D-GF and D-GT groups, a small number of immature gland-like structures formed in the wound area, indicating incomplete wound healing. Compared with the normal skin structure of rats, the newly formed wound area in the D-GT-DA group was basically close to the normal skin structure, and had functions such as hair growth

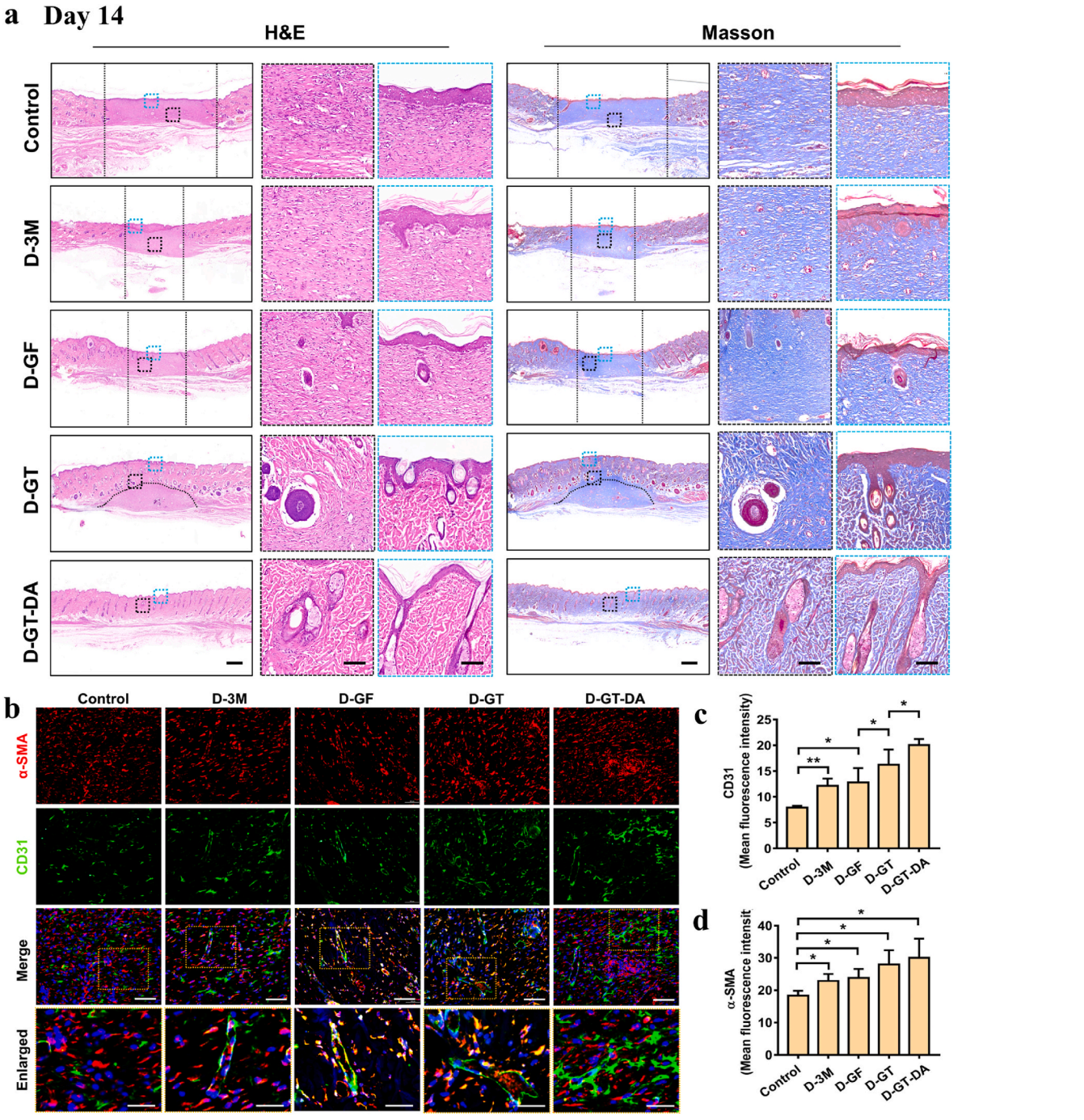

Fig. 5. Histological evaluation of skin wound healing process. (a) The H&E and Masson staining images of wounds in five groups on day 14 after dressing treatment. The enlarged image showed new skin structures such as the epidermis and hair follicles. Scale bars: 700 μm (left column) and 100 μm (right column). (b) Immunofluorescence staining of regenerated skin tissue labeled with CD31 and α-SMA. (c–d) Semi-quantitative analysis of CD31 and α-SMA proteins. Scale bars: 100 μm (merge regions) and 50 μm (enlarged regions). $^{*}P < 0.05$, $^{**}P < 0.01$.

and perspiration. As shown in Fig. 5a, a large number of blood vessels and hair follicles were formed, and their number and maturity were significantly better than those of the other four groups, indicating that the D-GT-DA group dressing had the strongest healing effect. By comparing D-GT and D-GF dressings, it can be concluded that the breathability of dressings was a crucial factor affecting skin wound healing. These results suggested that in addition to early inhibition of bacterial reproduction, wound dressing, and hemostasis, skin moisturization, and ventilation are also critical during wound healing.

Subsequently, we further performed immunofluorescence staining and semi-quantitative analysis of vascular-associated protein (CD31) and α-smooth muscle actin (α-SMA) to assess the angiogenesis of wound samples on day 14 (Fig. 5b–d). CD31, a transmembrane protein, plays an important role in regulating angiogenesis. On day 14, we observed that the expressions of CD31 in the four groups covered with dressings were notably higher than that in the control group. In addition, the expressions of CD31 in the D-GT-DA were the highest, indicating that glyhydrogel textile dressings with antibacterial, moisturizing, and ventilation functions had the best capability to promote tissue regeneration, and were the most suitable group for dressing infectious wounds. α-SMA is a marker of smooth muscle cell differentiation and one of the main elements constituting the cytoskeleton. In Fig. 5b, the control group, D-3M and D-GF groups showed a small amount of red positive areas. The red positive staining in D-GT and D-GT-DA groups was significantly higher than the other three groups. Among them, the red fluorescence intensity of the D-GT-DA group was the highest, which indicated that the angiogenic response of the D-GT-DA group was activated earlier in the wound healing process. In this study, glycerin was introduced into the dressing design to prepare a porous braided structure, which enabled the dressing to have both continuous moisturizing and breathable effects, and does not freeze in a cold environment. Therefore, it was expected to be prepared as a medical dressing and applied to infectious wounds even in cold regions.

4. Conclusion

In this work, we create a glyhydrogel textile as a new type of wound dressing featuring excellent breathability, antibacterium, antifreezing, and stretchability, which are hard to achieve in existing dressings. Accordingly, the glyhydrogel textile exhibits outstanding performance in treating infected wound and would be favorable for a wide range of applications including tissue protection, regenerative medicine, and wearable medical devices. The key element in this new dressing is hydrogel fibers, whose fabrication method remains a challenge. Here, we establish a mild while efficient wet spinning process based on the salting-out effect to continuously produce pure gelatin fiber without chemical modification at room temperature, which represents a new green strategy to enable a series of advanced fabrication including spinning, 3D printing, and microfluidic of biomacromolecule-based materials. Furthermore, the strategy of imparting the intrinsically antibacterial and the capacity of loading lipid-soluble components to materials by introducing glycerin is facile, efficient, universal, and can inspire a series of novel biomedical materials and treatments.

Ethics approval and consent to participate

All procedures were performed following the guidelines issued by the Animal Care and Use Committee of Shanghai Shengchang Biotechnology Co., Ltd (ethical code:2021-09-KQ-PJ-008).

CRediT authorship contribution statement

Sihan Jiang: Conceptualization, Writing – original draft, Writing – review & editing, Software, Methodology, Investigation, Validation, Formal analysis. **Jiajia Deng:** Writing – original draft, Writing – review & editing, Software, Methodology, Investigation, Validation, Formal analysis. **Yuhui Jin:** Data curation, Methodology, Visualization. **Bo Qian:** Data curation, Methodology, Visualization. **Wanqi Lv:** Data curation, Methodology, Visualization. **Qiangqiang Zhou:** Data curation, Methodology, Visualization. **Enhua Mei:** Data curation, Methodology, Visualization. **Rasoul Esmaeely Neisiany:** Writing – review & editing, Writing – review & editing, Writing – review & editing, Writing – review & editing, Writing – review & editing. **Yuehua Liu:** Writing – review & editing, Resources, Supervision. **Zhengwei You:** Conceptualization, Funding acquisition, Writing – review & editing, Resources, Project administration, Supervision. **Jie Pan:** Conceptualization, Funding acquisition, Writing – review & editing, Resources, Project administration, Supervision.

Declaration of competing interest

The authors declare no conflict of interest.

Acknowledgements

We thank Professor Li Jiyang, School of Pharmacy, Fudan University, for providing us with Staphylococcus aureus and experimental guidance. This study was financially supported by the National Key Research and Development Program of China (2021YFC2101800, 2021YFC2400802), the National Natural Science Foundation of China (52173117), the Natural Science Foundation of Shanghai (20ZR1402500), Belt & Road Young Scientist Exchanges Project of Science and Technology Commission Foundation of Shanghai (20520741000), Ningbo 2025 Science and Technology Major Project (2019B10068), Science and Technology Commission of Shanghai Municipality (20DZ2254900, 20DZ2270800), the Fundamental Research Funds for the Central Universities, DHU Distinguished Young Professor Program (LZA2019001), Shanghai Stomatological Hospital Science and Technology Talents Project (SSH-2022-KJCX-B01).

Appendix A. Supplementary data

Supplementary data to this article can be found online at https://doi.org/10.1016/j.bioactmat.2022.08.014.

References

[1] S. MacNeil, Progress and opportunities for tissue-engineered skin, Nature 445 (2007) 874–880.
[2] M. Rodrigues, N. Kosaric, C.A. Bonham, G.C. Gurtner, Wound healing: a cellular perspective, Physiol. Rev. 99 (2019) 665–706.
[3] Y. Dong, Y. Zheng, K. Zhang, Y. Yao, L. Wang, X. Li, J. Yu, B. Ding, Electrospun nanofibrous materials for wound healing, Adv. Fiber Mater. 2 (2020) 212–227.
[4] U. Park, M.S. Lee, J. Jeon, S. Lee, M.P. Hwang, Y. Wang, H.S. Yang, K. Kim, Coacervate-mediated exogenous growth factor delivery for scarless skin regeneration, Acta Biomater. 90 (2019) 179–191.
[5] P. Pleguezuelos-Beltran, P. Galvez-Martin, D. Nieto-Garcia, J.A. Marchal, E. Lopez-Ruiz, Advances in spray products for skin regeneration, Bioact. Mater. 16 (2022) 187–203.
[6] P. Zahedi, I. Rezaeian, S.-O. Ranaei-Siadat, S.-H. Jafari, P. Supaphol, A review on wound dressings with an emphasis on electrospun nanofibrous polymeric bandages, Polym. Adv. Technol. 21 (2010) 77–95.
[7] X. Zhao, H. Wu, B. Guo, R. Dong, Y. Qiu, P.X. Ma, Antibacterial anti-oxidant electroactive injectable hydrogel as self-healing wound dressing with hemostasis and adhesiveness for cutaneous wound healing, Biomaterials 122 (2017) 34–47.
[8] M. Farokhi, F. Mottaghitalab, Y. Fatahi, A. Khademhosseini, D.L. Kaplan, Overview of silk fibroin use in wound dressings, Trends Biotechnol. 36 (2018) 907–922.
[9] X. Ding, G. Li, P. Zhang, E. Jin, C. Xiao, X. Chen, Injectable self-healing hydrogel wound dressing with cysteine-specific on-demand dissolution property based on tandem dynamic covalent bonds, Adv. Funct. Mater. 31 (2021), 2011230.
[10] S. Matoori, A. Veves, D.J. Mooney, Advanced bandages for diabetic wound healing, Sci. Transl. Med. 13 (2021), eabe4839.
[11] H. Wang, Z. Xu, M. Zhao, G. Liu, J. Wu, Advances of hydrogel dressings in diabetic wounds, Biomater. Sci. 9 (2021) 1530–1546.
[12] W.C. Huang, R. Ying, W. Wang, Y. Guo, Y. He, X. Mo, C. Xue, X. Mao, A macroporous hydrogel dressing with enhanced antibacterial and anti-inflammatory capabilities for accelerated wound healing, Adv. Funct. Mater. 30 (2020), 2000644.

[13] Z. Zhu, S. Ling, J. Yeo, S. Zhao, L. Tozzi, M.J. Buehler, F. Omenetto, C. Li, D. L. Kaplan, High-strength, durable all-silk fibroin hydrogels with versatile processability toward multifunctional applications, Adv. Funct. Mater. 28 (2018), 1704757.
[14] Y. Yang, Y. Liang, J. Chen, X. Duan, B. Guo, Mussel-inspired adhesive antioxidant antibacterial hemostatic composite hydrogel wound dressing via photo-polymerization for infected skin wound healing, Bioact. Mater. 8 (2022) 341–354.
[15] L. Zeng, J. He, Y. Cao, J. Wang, Z. Qiao, X. Jiang, L. Hou, J. Zhang, Tissue-adhesive and highly mechanical double-network hydrogel for cryopreservation and sustained release of anti-cancer drugs, Smart Mater. Med. 2 (2021) 229–236.
[16] L. Sun, H. Huang, Q. Ding, Y. Guo, W. Sun, Z. Wu, M. Qin, Q. Guan, Z. You, Highly transparent, stretchable, and self-healable ionogel for multifunctional sensors, triboelectric nanogenerator, and wearable fibrous electronics, Adv. Fiber Mater. 4 (2022) 98–107.
[17] N. Yang, P. Qi, J. Ren, H. Yu, S. Liu, J. Li, W. Chen, D.L. Kaplan, S. Ling, Polyvinyl alcohol/silk fibroin/borax hydrogel ionotronics: a highly stretchable, self-healable, and biocompatible sensing platform, ACS Appl. Mater. Interfaces 11 (2019) 23632–23638.
[18] A. Miyamoto, S. Lee, N.F. Cooray, S. Lee, M. Mori, N. Matsuhisa, H. Jin, L. Yoda, T. Yokota, A. Itoh, M. Sekino, H. Kawasaki, T. Ebihara, M. Amagai, T. Someya, Inflammation-free, gas-permeable, lightweight, stretchable on-skin electronics with nanomeshes, Nat. Nanotechnol. 12 (2017) 907–913.
[19] W. Yang, N.-W. Li, S. Zhao, Z. Yuan, J. Wang, X. Du, B. Wang, R. Cao, X. Li, W. Xu, Z.L. Wang, C. Li, A breathable and screen-printed pressure sensor based on nanofiber membranes for electronic skins, Adv. Mater. Technol. 3 (2018), 1700241.
[20] Y. Liu, W.M. Au, H. Hu, Protective properties of warp-knitted spacer fabrics under impact in hemispherical form. Part i: impact behavior analysis of a typical spacer fabric, Textil. Res. J. 84 (2013) 422–434.
[21] R.D. Pedde, B. Mirani, A. Navaei, T. Styan, S. Wong, M. Mehrali, A. Thakur, N. K. Mohtaram, A. Bayati, A. Dolatshahi-Pirouz, M. Nikkhah, S.M. Willerth, M. Akbari, Emerging biofabrication strategies for engineering complex tissue constructs, Adv. Mater. 29 (2017), 1606061.
[22] R. Bagherzadeh, M. Gorji, M. Latifi, P. Payvandy, L.X. Kong, Evolution of moisture management behavior of high-wicking 3d warp knitted spacer fabrics, Fibers Polym. 13 (2012) 529–534.
[23] M. Akbari, A. Tamayol, S. Bagherifard, L. Serex, P. Mostafalu, N. Faramarzi, M. H. Mohammadi, A. Khademhosseini, Textile technologies and tissue engineering: a path toward organ weaving, Adv. Healthcare Mater. 5 (2016) 751–766.
[24] H. Wang, H. Liu, X. Zhang, Y. Wang, M. Zhao, W. Chen, J. Qin, One-step generation of aqueous-droplet-filled hydrogel fibers as organoid carriers using an all-in-water microfluidic system, ACS Appl. Mater. Interfaces 13 (2021) 3199–3208.
[25] G.H. Dayan, N. Mohamed, I.L. Scully, D. Cooper, E. Begier, J. Eiden, K.U. Jansen, A. Gurtman, A.S. Anderson, Staphylococcus aureus: the current state of disease, pathophysiology and strategies for prevention, Expert Rev. Vaccines 15 (2016) 1373–1392.
[26] E.Y. Klein, T.P. Van Boeckel, E.M. Martinez, S. Pant, S. Gandra, S.A. Levin, H. Goossens, R. Laxminarayan, Global increase and geographic convergence in antibiotic consumption between 2000 and 2015, Proc. Natl. Acad. Sci. U.S.A. 115 (2018) E3463–E3470.
[27] Q. Pang, D. Lou, S. Li, G. Wang, B. Qiao, S. Dong, L. Ma, C. Gao, Z. Wu, Smart flexible electronics-integrated wound dressing for real-time monitoring and on-demand treatment of infected wounds, Adv. Sci. 7 (2020), 1902673.
[28] X. Wang, C. Han, X. Hu, H. Sun, C. You, C. Gao, Y. Haiyang, Applications of knitted mesh fabrication techniques to scaffolds for tissue engineering and regenerative medicine, J. Mech. Behav. Biomed. Mater. 4 (2011) 922–932.
[29] L. Han, K. Liu, M. Wang, K. Wang, L. Fang, H. Chen, J. Zhou, X. Lu, Mussel-inspired adhesive and conductive hydrogel with long-lasting moisture and extreme temperature tolerance, Adv. Funct. Mater. 28 (2018), 1704195.
[30] D. Li, K. Chen, H. Tang, S. Hu, L. Xin, X. Jing, Q. He, S. Wang, J. Song, L. Mei, R. D. Cannon, P. Ji, H. Wang, T. Chen, A logic-based diagnostic and therapeutic hydrogel with multistimuli responsiveness to orchestrate diabetic bone regeneration, Adv. Mater. 34 (2022), 2108430.
[31] P.N. Bernal, M. Bouwmeester, J. Madrid-Wolff, M. Falandt, S. Florczak, N. G. Rodriguez, Y. Li, G. Grossbacher, R.A. Samsom, M. van Wolferen, L.J.W. van der Laan, P. Delrot, D. Loterie, J. Malda, C. Moser, B. Spee, R. Levato, Volumetric bioprinting of organoids and optically tuned hydrogels to build liver-like metabolic biofactories, Adv. Mater. 34 (2022), 2110054.
[32] B. Park, J.H. Shin, J. Ok, S. Park, W. Jung, C. Jeong, S. Choy, Y.J. Jo, T.I. Kim, Cuticular pad-inspired selective frequency damper for nearly dynamic noise-free bioelectronics, Science 376 (2022) 624–629.
[33] C.Q. Sun, Y. Huang, X. Zhang, Hydration of hofmeister ions, Adv. Colloid Interface Sci. 268 (2019) 1–24.
[34] D. Chandler, Interfaces and the driving force of hydrophobic assembly, Nature 437 (2005) 640–647.
[35] Q. He, Y. Huang, S. Wang, Hofmeister effect-assisted one step fabrication of ductile and strong gelatin hydrogels, Adv. Funct. Mater. 28 (2018), 1705069.
[36] S. Bertlein, G. Brown, K.S. Lim, T. Jungst, T. Boeck, T. Blunk, J. Tessmar, G. J. Hooper, T.B.F. Woodfield, J. Groll, Thiol-ene clickable gelatin: a platform bioink for multiple 3d biofabrication technologies, Adv. Mater. 29 (2017), 1703404.
[37] N. Cebi, M.Z. Durak, O.S. Toker, O. Sagdic, M. Arici, An evaluation of fourier transforms infrared spectroscopy method for the classification and discrimination of bovine, porcine and fish gelatins, Food Chem. 190 (2016) 1109–1115.
[38] Z. Qin, X. Sun, H. Zhang, Q. Yu, X. Wang, S. He, F. Yao, J. Li, A transparent, ultrastretchable and fully recyclable gelatin organohydrogel based electronic sensor with broad operating temperature, J. Mater. Chem. 8 (2020) 4447–4456.
[39] X. Cui, J. Lee, K.R. Ng, W.N. Chen, Food waste durian rind-derived cellulose organohydrogels: toward anti-freezing and antimicrobial wound dressing, ACS Sustainable Chem. Eng. 9 (2021) 1304–1312.
[40] J. Song, S. Chen, L. Sun, Y. Guo, L. Zhang, S. Wang, H. Xuan, Q. Guan, Z. You, Mechanically and electronically robust transparent organohydrogel fibers, Adv. Mater. 32 (2020), 1906994.
[41] R. Youssef, V. Hafez, Y. Elkholy, A. Mourad, Glycerol 85% efficacy on atopic skin and its microbiome: a randomized controlled trial with clinical and bacteriological evaluation, J. Dermatol. Treat. 32 (2021) 730–736.
[42] V.S. Saegeman, N.L. Ectors, D. Lismont, B. Verduyckt, J. Verhaegen, Short- and long-term bacterial inhibiting effect of high concentrations of glycerol used in the preservation of skin allografts, Burns 34 (2008) 205–211.
[43] C.P. Parlet, M.M. Brown, A.R. Horswill, Commensal staphylococci influence staphylococcus aureus skin colonization and disease, Trends Microbiol. 27 (2019) 497–507.
[44] H. Lei, C. Zhu, D. Fan, Optimization of human-like collagen composite polysaccharide hydrogel dressing preparation using response surface for burn repair, Carbohydr. Polym. 239 (2020), 116249.
[45] Y. Liu, H. Hu, W.M. Au, Protective properties of warp-knitted spacer fabrics under impact in hemispherical form. Part ii: effects of structural parameters and lamination, Textil. Res. J. 84 (2013) 312–322.
[46] S.P. Lacour, G. Courtine, J. Guck, Materials and technologies for soft implantable neuroprostheses, Nat. Rev. Mater. 1 (2016), 16063.
[47] Y. Yu, H. Yuk, G.A. Parada, Y. Wu, X. Liu, C.S. Nabzdyk, K. Youcef-Toumi, J. Zang, X. Zhao, Multifunctional "hydrogel skins" on diverse polymers with arbitrary shapes, Adv. Mater. 31 (2019), 1807101.
[48] X. Zhao, Y. Zhou, J. Xu, G. Chen, Y. Fang, T. Tat, X. Xiao, Y. Song, S. Li, J. Chen, Soft fibers with magnetoelasticity for wearable electronics, Nat. Commun. 12 (2021) 6755.
[49] J. Zhao, Y. Tang, Y. Liu, L. Cui, X. Xi, N. Zhang, P. Zhu, Design carboxymethyl cotton knitted fabrics for wound dressing applications: solvent effects, Mater. Des. 87 (2015) 238–244.
[50] H.M. Fahmy, A.A. Aly, A. Abou-Okeil, A non-woven fabric wound dressing containing layer - by - layer deposited hyaluronic acid and chitosan, Int. J. Biol. Macromol. 114 (2018) 929–934.
[51] F. Ahmad, B. Mushtaq, F.A. Butt, M.S. Zafar, S. Ahmad, A. Afzal, Y. Nawab, A. Rasheed, Z. Ulker, Synthesis and characterization of nonwoven cotton-reinforced cellulose hydrogel for wound dressings, Polymers 13 (2021) 4098.
[52] R. Uppal, G.N. Ramaswamy, C. Arnold, R. Goodband, Y. Wang, Hyaluronic acid nanofiber wound dressing—production, characterization, and in vivo behavior, J. Biomed. Mater. Res. B 97 (2011) 20–29.
[53] Y. Yang, H. Hu, Application of superabsorbent spacer fabrics as exuding wound dressing, Polymers 10 (2018) 210.
[54] G.C. Türkoğlu, A.M. Sarıışık, S.Y. Karavana, Development of textile-based sodium alginate and chitosan hydrogel dressings, Int. J. Polym. Mater. Polym. Biomater. 70 (2020) 916–925.
[55] R. Nawalakhe, Q. Shi, N. Vitchuli, J. Noar, J.M. Caldwell, F. Breidt, M.A. Bourham, X. Zhang, M.G. McCord, Novel atmospheric plasma enhanced chitosan nanofiber/gauze composite wound dressings, J. Appl. Polym. Sci. 129 (2013) 916–923.
[56] Y. Liang, Z. Li, Y. Huang, R. Yu, B. Guo, Dual-dynamic-bond cross-linked antibacterial adhesive hydrogel sealants with on-demand removability for post-wound-closure and infected wound healing, ACS Nano 15 (2021) 7078–7093.